OncoTargets and Therapy

Dovepress
open access to scientific and medical research

Open Access Full Text Article

ORIGINAL RESEARCH

The inhibitive effect of sh-HIF1A-AS2 on the proliferation, invasion, and pathological damage of breast cancer via targeting miR-548c-3p through regulating HIF-1α/VEGF pathway in vitro and vivo

This article was published in the following Dove Medical Press journal:
OncoTargets and Therapy

Xiao Guo[1,*]
Shenghai Lee[2,*]
Peilong Cao[3]

[1]Department of Breast Surgery, Central Clinical College of Gynecology Obstetrics, Tianjin Medical University, Tianjin 300110, China; [2]Department of Surgery, Zhaoqing Medical College, Zhaoqing, Guangdong 526020, China; [3]Department of Pathology, The First Affiliated Hospital of Xi'an Jiaotong University, Xi'an, Shanxi 710061, China

*These authors contributed equally to this work

Background: Breast cancer (BC) has been the commonest malignant tumor with a low survival rate among woman. Long non-coding RNA hypoxia-inducible factor-1 alpha antisense RNA-2 (HIF1A-AS2) was correlated with various cancers.

Purpose: The study aimed to investigate the role and related underlying molecular mechanisms of HIF1A-AS2 in BC.

Material and methods: Target relationships were speculated by Targetscan 7.0 and confirmed by dual luciferase reporter assay. Proteins levels were monitored by RT-qPCR, Western blot and immunohistochemistry assay. CCK-8 assay, SA-β-gal staining and transwell assay were used to detect proliferation, senescence and invasion, respectively. Xenograft nude mice were put into use to evaluate the tumor growth and motility.

Results: The present study exhibited that HIF1A-AS2 and hypoxia-inducible factor-1 alpha (HIF-1α) were upregulated while miR-548c-3p was downregulated in MDA-MB-231, MCF-7, ZR-75-1, and MDA-MB-549 BC cell lines. Bioinformatics analysis showed HIF1A-AS2 and HIF-1α were the targets of miR-548c-3p, and the target relationship was further confirmed by dual luciferase reporter assay. Moreover, knockdown of HIF1A-AS2 by shRNA (sh-HIF1A-AS2) markedly elevated miR-548c-3p level, and the enhanced miR-548c-3p noticeably suppressed cell proliferation, invasion, and epithelial–mesenchymal transition, and promoted senescence in vitro. In addition, overexpression of HIF-1α promoted MCF-7 cell invasion. Intriguingly, low expression of HIF1A-AS2 reduced HIF-1α level by upregulating the expression of miR-548c-3p. Furthermore, experiment in xenograft nude mice has indicated that sh-HIF1A-AS2 inhibited tumor growth and motility by targeting miR-548c-3p through regulating HIF-1α/vascular endothelial growth factor (VEGF) pathway in vivo.

Conclusion: The inhibitive effect of HIF-1α/VEGF pathway by sh-HIF1A-AS2 through targeting miR-548c-3p plays crucial regulatory roles in BC. Therefore, designing targeted drugs against HIF1A-AS2 provides a new direction for the treatment of BC.

Keywords: breast cancer, oncogenesis, HIF1A-AS2, miR-548c-3p, HIF-1α/VEGF, MCF-7

Introduction

Breast cancer (BC), one of the most common malignant tumors in women, is derived from breast tissue and has become a foremost cause of death among woman. In China, the morbidity of BC has reached 15%.[1–3] Approximately 90% of BC lethality is attributed to the metastasis and the immunity of current therapeutics.[4–6] Despite the widespread application of adjunctive therapies, the survival rates of BC patients remain low.[7] Recently, immunotherapy has elevated the rehabilitation to some extent.

Correspondence: Peilong Cao
Department of Pathology, The First Affiliated Hospital of Xi'an Jiaotong University, No 277 Yanta West Road, Yanta District, Xi'an, Shanxi Province, China
Tel +86 176 6503 6839
Email ypeilongcaoxq@sina.com

submit your manuscript | www.dovepress.com
Dovepress
http://dx.doi.org/10.2147/OTT.S192377

Nevertheless, there is still an urgent need to investigate the potential molecular mechanism of BC to explore more effective therapies for the treatment of BC.[8]

Numerous studies have demonstrated that long noncoding RNAs (lncRNAs) play a critical role in regulation[9,10] and tumorigenesis.[11–13] Hypoxia-inducible factor-1 alpha antisense RNA-2 (HIF1A-AS2), an antisense lncRNA (aslncRNA), was proved to be a natural antisense transcript of hypoxia-inducible factor-1alpha (HIF-1α).[14] Many studies have indicated that HIF1A-AS2 is associated with a variety of cancers,[15] such as gastric cancer,[16] bladder cancer,[17] ischemic stroke,[18] and colorectal cancer.[19] However, the roles and molecular mechanisms of HIF1A-AS2 in BC are still unclear.

Hypoxia is usually witnessed in the tumor environment once the cell growth takes place rapidly.[20] HIF-1α, an oxygen-sensitive transcription factor, enables the transcription of multifarious proangiogenic cytokines such as vascular endothelial growth factor (VEGF). It has been reported that HIF-1α-mediated VEGF signaling pathway plays a crucial role in breast tumorigenesis.[21] Previous studies showed that accumulation of HIF-1α under ischemic and hypoxic conditions contributed to the inhibitive effect of degradation mediated by ubiquitination. Additionally, a novel evidence was presented that HIF-1α abundance was controlled by miRNA as well.[

miR-548c is a member of miR-548 which originated from a inverted repeat transposition element. The mature miR-548c-3p is obtained from miR-548c and consists of 22 nucleotides. A mass of studies have indicated that miR-548c-3p is involved in various cancers, including prostate cancer,[23] glioma,[24] gastric cancer,[25] and BC.[26] Nevertheless, the underlying molecular mechanisms of miR-548c-3p in BC remain undiscovered.

This study aimed to investigate the roles and related underlying molecular mechanisms of HIF1A-AS2 in BC in vivo and vitro. In the present study, we revealed a novel mechanism of HIF1A-AS2 in tumorigenesis of BC, asserting that designing targeted drugs against HIF1A-AS2 provide a new direction for the treatment of BC.

Materials and methods

Cell lines and cell culture

Four BC cell lines (MDA-MB-231, MCF-7, ZR-75-1, BT-549) and immortalized normal BC cell line MCF-10A were purchased from the Type Culture Collection of the Chinese Academy of Science. (Shanghai, China). MCF-10A cells were cultured in DMEM (Thermo Fisher Scientific, Waltham, MA, USA) containing 10 mg/mL $NaHCO_3$. ZR-75-1 cells were cultured in DMEM supplemented with 10% FBS, 0.37% $NaHCO_3$, 10 mM 2-(4-[2-hydroxyethyl]-1-piperazinyl) ethanesulfonic acid, 100 U/mL penicillin, and 1 μg/mL streptomycin (Thermo Fisher Scientific). MCF-7 and BT-549 cells were cultured in Roswell Park Memorial Institute-1640 medium including 10% FBS, 0.2% $NaHCO_3$, 10 mM 2-(4-[2-Hydroxyethyl]-1-piperazinyl) ethanesulfonic acid, 100 U/mL penicillin, and 1 μg/mL streptomycin, pH 7.2 (Thermo Fisher Scientific). MDA-MB-231 cells were cultured in Leibovitz medium (L-15) with 10% FBS, 100 U/mL penicillin, and 1 μg/mL streptomycin, pH 7.2 (Thermo Fisher Scientific). All cells were cultivated at 37°C with 5% CO_2. To investigate the interaction between HIF1A-AS2 and HIF-1α, cells were incubated in an atmosphere containing 1% O_2 and 5% CO_2 at 37°C.

Cell transfection

sh-HIF1A-AS2, Ad-HIF1A-AS2, pLenti-CMV-HIF-1α, miR-548c-3p inhibitor, miR-548c-3p mimic, and negative control were provided by Gene Pharma (Shanghai, China). Transfection of MCF-7 cells was conducted using Lipofectamine 2000 transfection reagent (Thermo Fisher Scientific). Cells were cultured in six-well plates for 48 hours and collected for subsequent analyses.

Reverse transcription quantitative real-time PCR (RT-qPCR)

Total RNAs were extracted from MDA-MB-231, MCF-7, ZR-75-1, BT-549, MCF-10A, and tumor tissues with Trizol reagent (Thermo Fisher Scientific) and reverse-transcribed to cDNA by RevertAid First Strand cDNA Synthesis kit (Thermo Fisher Scientific). RT-qPCR was conducted by SYBR-Green PCR Master Mix kit (Takara, Tokyo, Japan) and ABI 7500 Real-Time PCR System (Thermo Fisher Scientific). All operations were carried out in accordance with the corresponding instructions.

The primers of GAPDH were 5′-GTCAGGATCCACTCATCACG-3′ (sense) and 5′-GATCGGACTTACGGACTCACATC-3′ (antisense). The primers of β-actin were 5′-TCACCGAGCGCGGCT-3′ (sense) and 5′-TAATGTCACGCACGATTTCCC-3′ (antisense). The primers of HIF1A-AS2 were 5′-TGATCCAGTCAAAGATTCGCA-3′ (sense) and 5′-TCCATGATGCCAGCTCGATCTCACAG-3′ (antisense). The primers of miR-548c-3p were 5′-TGTCCTTAGCACCTGGTACGGACCGCT-3′ (sense) and 5′-TGCAATCTGGACTACCGATGG-3′ (antisense). The primers of HIF-1α were 5′-AGTAATCGGACTACCGGACGTG-3′ (sense) and 5′-TGGGCATTACATCGCATGCATC-3′ (antisense). GAPDH and β-actin were used as internal references. Fold changes were calculated by the equation $2^{-\Delta\Delta Ct}$. All experiments were repeated three times.

Dual luciferase reporter assay

Targetscan7.0 (http://www.targetscan.org) was used to predict the target of miR-548c-3p on the lncRNA HIF1A-AS2 3′untranslated region (3′UTR). The 3′UTR segments of HIF1A-AS2 (wild type [wt] and mutant [mut]) were amplified and inserted into the luciferase reporter vector (pmirGLO; Promega Corporation, Fitchburg, WI, USA). MCF-7 cells (8×10^4 cells/well) were transfected with Luc-HIF1A-AS2-wt, Luc-HIF1A-AS2-mut, or in combination with miRNA-548c using Lipofectamine 2000 transfection reagent (Thermo Fisher Scientific). The luciferase activities were detected by Dual-Luciferase Reporter Assay kit (Promega Corporation). All experiments were repeated three times.

Western blot analysis

MCF-7 cells and tumor tissues were ground in liquid nitrogen and lysed in lysis buffer (Beyotime, Shanghai, China). After separation by 8% SDS poly-acrylamide gel, the objective proteins were transferred to polyvinylidene difluoride membranes (IPFL00010; EMD Millipore, Billerica, MA, USA). Primary antibodies specific to Ki-67 (sc-23900, 1:1,000), VEGF (sc-7269, 1:1,000), PCNA (sc-71858, 1:1,000), E-cadherin (sc-8426, 1:1,000), vimentin (sc-80975, 1:1,000), N-cadherin (sc-8424, 1:1,000), [illegible] (sc-13515, 1:1,000), and GAPDH (sc-66163, 1:1,000) were applied. Then, the samples were incubated with second antibodies (sc-516102; Santa Cruz Biotechnology Inc, Dallas, TX, USA) and detected with [illegible] enhanced chemiluminescence substrate kit (Amersham Biosciences). The relative protein level was analyzed by using ImageJ software. All experiments were repeated three times.

Cell proliferation

Proliferative ability of MCF-7 cells was measured by Cell Counting Kit-8 (CCK-8) (Dojindo, Kumamoto, Japan) according to the manufacturer's protocol. MCF-7 cells were transfected with sh-HIF1A-AS2 or miR-548c inhibitor and in combination with miR-548c inhibitor and incubated in 10% CCK-8 at 37°C for 3 hours. Proliferation rates were measured at 0, 1, 2, 3, and 4 days, respectively. The absorbance was determined at 570 nm with multifunctional microplate reader SpectraMax M5 (Molecular Devices, Sunnyvale, CA, USA). All experiments were repeated three times.

Cell senescence

Cell senescence was measured with the senescence-associated β-galactosidase (SA-β-gal) staining kit (Beyotime) according to the manufacturer's protocol. All experiments were repeated three times.

Transwell assay

Transwell assay was conducted to monitor the invasive capacity of tumor cells. Matrigel was coated on the surface of the upper chamber after diluting with serum-free DMEM medium. This was air dried at room temperature for later use. After starving the culture with serum-free medium for 24 hours, the cell suspension was transferred to the apical chambers (200 mL per chamber). The lower chambers were loaded with 600 μL of medium containing 10% FBS. After incubation at 37°C for 48 hours, the chambers were pulled out and washed with PBS. A cotton bud was used to [illegible] the residual cells on the upper membranes. After fixing with [illegible]% alcohol and staining with crystal violet, the cells were photographed under a microscope (Leica Microsystems, Wetzlar, Germany). The experiments were independently repeated in triplicate.

Animal model

All animal experiments were performed in accordance with the National Institutes of Health Guide for the Care and Use of Laboratory Animals and were approved by the Central Clinical College of Gynecology Obstetrics of Tianjin Medical University. A total of 10 BALB/c nude mice (male, 4-week-old) were obtained from the Animal Center of Tianjin Medical University and housed in a controlled environment at 25°C±3°C and 60% humidity, in a 12-hour light/dark cycle with free access to food and water. Untreated MCF-7 cells or MCF-7 cells (2×10^5) transfected with sh-HIF1A-AS2 were subcutaneously injected into the flank area of mice to form tumors. After successful modeling, mice were divided into two groups with ten in each group (repeat three times): control group and sh-HIF1A-AS2 group (mice injected with MCF-7 cells transfected with sh-HIF1A-AS2). Tumor weight was measured at 25 days post-injection. After 25 days, rats were euthanized by intraperitoneal injection of pentobarbital sodium (200 mg/kg body weight). Tumors were collected for the following experiments.

Immunohistochemistry (IHC)

IHC analysis was performed according to a previously described method.[27] Briefly, 5 μm thick paraffin sections were deparaffinized in xylene and rehydrated in ethanol at different gradients. After that, the tissue slices were incubated in 30% H_2O_2 for 30 minutes to inactivate endogenous peroxidase. After antigen retrieval in 10 mM heated citrate buffer for 10 minutes, the tissue sections were incubated with primary antibodies Ki-67 (#9027, 1:400; CST, St Louis, MO, USA) and VEGF (#9698, 1:1600; CST) overnight at 4°C. Corresponding secondary antibody (#8114; CST) was added and incubated for 1 hour at room temperature. The images were observed under a microscope (E200; Nikon, Tokyo, Japan).

Statistical analysis

The statistical analysis was conducted with SPSS 21.0 (SPSS, Inc, Chicago, IL, USA). Measurement data were presented as mean ± SD (x±s), and data consistent with the normal distribution were analyzed by independent *t*-test. Multiple sets of data were analyzed by one-way ANOVA followed by Bonferroni post hoc test. Enumeration data were presented as a percentage or ratio and verified with chi-squared test. $P<0.05$ was considered statistically significant.

Results

Increase of HIF1A-AS2 and decrease of miR-548c-3p in human BC cells

RT-qPCR was conducted to monitor the expression levels of HIF1A-AS2 and miR-548c-3p. As shown in Figure 1A, HIF1A-AS2 was significantly increased in four BC cell lines (MDA-MB-231, MCF-7, ZR-75–1, and BT-549) compared with normal mammary epithelial cell line (MCF-10A) ($P<0.05$, $P<0.01$), whereas miR-548c-3p was significantly decreased (Figure 1B; $P<0.05$, $P<0.01$). MCF-7 cell line was used as the follow-up experimental cell line due to the high significant differences observed with MCF-10A ($P<0.01$). Taken together, these results demonstrated that HIF1A-AS2 and miR-548c-3p might be correlated with human BC with contrary effects.

miR-548c-3p targeted HIF1A-AS2 and was negatively regulated by HIF1A-AS2 in MCF-7 cells

Targetscan7.0 (http://www.targetscan.org) was used to predict the presumptive target of miR-548c-3p on HIF1A-AS2 3′UTR (wt and mut) (Figure 2A). miR-548c-3p was measured by RT-qPCR. As shown in Figure 2B, miR-548c-3p was noticeably upregulated in MCF-7 cells transfected with sh-HIF1A-AS2. A reversed result was observed while transfected with miR-548c-3p inhibitor (Figure 2B; $P<0.05$). Besides, overexpression of HIF1A-AS2 significantly inhibited the expression of miR-548c-3p (Figure 2C; $P<0.05$), whereas a reversed result was observed in MCF-7 cells transfected with miR-548c-3p mimic (Figure 2C; $P<0.001$). Furthermore, luciferase reporter assay further confirmed the correlation between HIF1A-AS2 and miR-548c-3p. The results of the luciferase reporter assay clearly showed a dramatic downregulation in luciferase activity (Figure 2D; $P<0.05$), while no marked effect was observed with the transfection of HIF1A-AS2 mut and miR-548c-3p mimic. These results demonstrated that miR-548c-3p targets HIF1A-AS2 3′UTR leading to the downregulation of luciferase activity (Figure 2D; $P<0.05$). In short, these results indicated that HIF1A-AS2 negatively regulated miR-548c-3p in MCF-7.

sh-HIF1A-AS2 suppressed proliferation and senescence by regulating miR-548c-3p in MCF-7 cells

CCK-8 assay was performed to investigate proliferation, while SA-β-gal staining was applied to investigate senescence and Western blot was used for further verification of cell proliferative potential. As shown in Figure 3A, results showed that proliferation capacity was significantly impeded in MCF-7 cells after transfection with sh-HIF1A-AS2 (Figure 3A; $P<0.05$, $P<0.01$). Meanwhile, Western blot

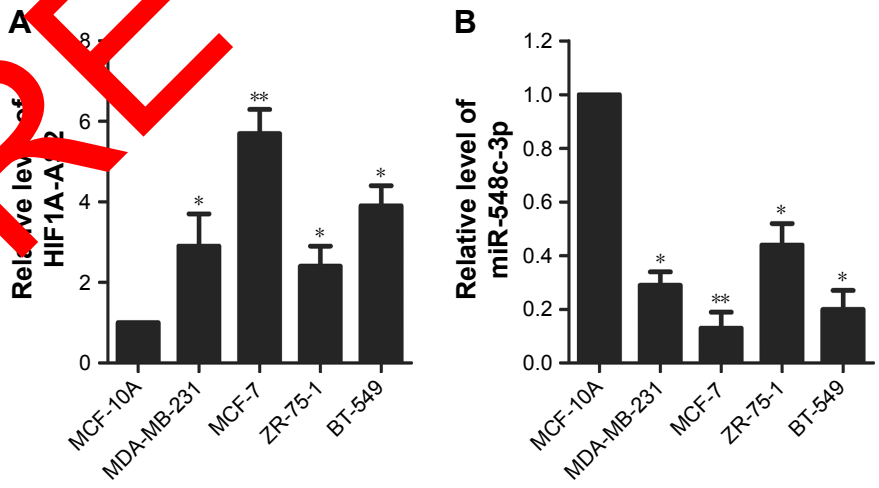

Figure 1 Increase of HIF1A-AS2 and decrease of miR-548c-3p in human BC cells.
Notes: (**A**) The expression level of HIF1A-AS2 was measured by RT-qPCR in MCF-10A and BC cell lines (MDA-MB-231, MCF-7, ZR-75-1, and BT-549). (**B**) The expression level of miR-548c-3p was detected by RT-qPCR in MCF-10A and BC cell lines (MDA-MB-231, MCF-7, ZR-75-1, and BT-549). *$P<0.05$ vs control; **$P<0.01$ vs control.
Abbreviations: BC, breast cancer; HIF1A-AS2, hypoxia-inducible factor-1 alpha antisense RNA-2; RT-qPCR, quantitative real-time PCR.

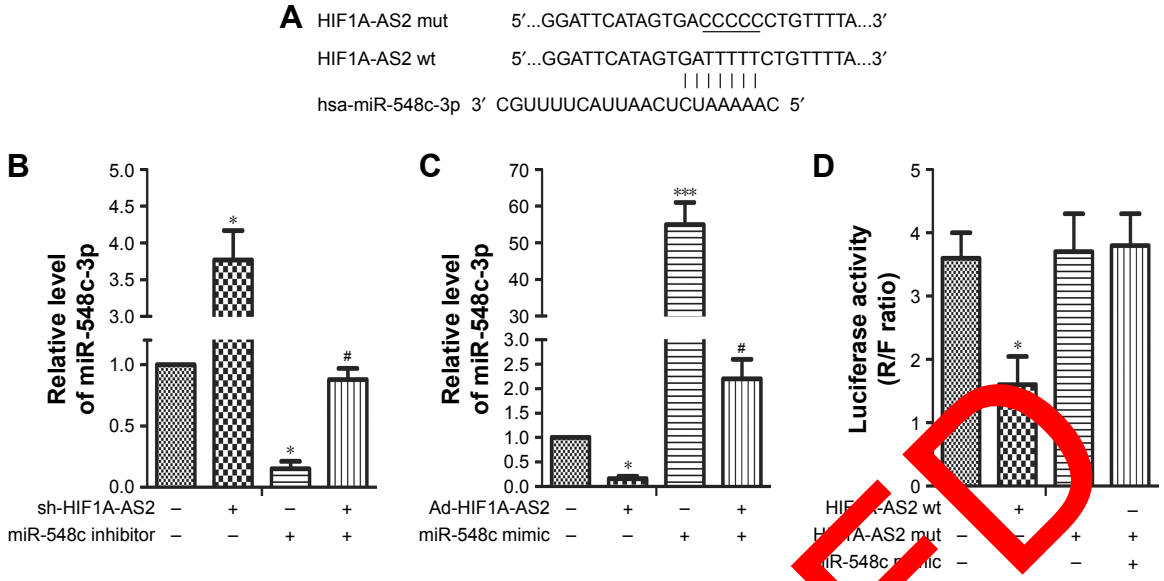

Figure 2 miR-548c-3p targeted HIF1A-AS2 and was negatively regulated by HIF1A-AS2 in MCF-7 cells.
Notes: (**A**) The target of miR-548c-3p on HIF1A-AS2 3′UTR (wt and mut). (**B**) The expression level of miR-548c-3p was detected by RT-qPCR in MCF-7 cells transfected with sh-HIF1A-AS2 or miR-548c inhibitor and in combination with miR-548c inhibitor (*$P<0.05$ vs control, #$P<0.05$ vs miR-548c inhibitor group). (**C**) The expression level of miR-548c-3p was detected by RT-qPCR in MCF-7 cells transfected with Ad-HIF1A-AS2 or miR-548c mimic and in combination with miR-548c mimic (*$P<0.05$ vs control, ***$P<0.001$ vs control, #$P<0.05$ vs miR-548c mimic group). (**D**) The activity of HIF1A-AS2 was measured by dual luciferase reporter assay in MCF-7 cells co-transfected with HIF1A-AS2 (wt and mut) and miR-548c mimics (*$P<0.05$ vs control). "R" represents the relative light unit of Renilla luciferase. "F" represents the relative light unit of Firefly luciferase.
Abbreviations: HIF1A-AS2, hypoxia-inducible factor-1 alpha antisense RNA-2; mut, mutant; RT-qPCR, quantitative real-time PCR; UTR, untranslated region; wt, wild type.

assays exhibited that the proliferation marker proteins levels (Ki-67 and PCNA) were downregulated in MCF-7 cells after transfection with sh-HIF1A-AS2, and the inhibition was counteracted by miR-548c-3p inhibitor (Figure 3C and D; $P<0.05$). Besides, SA-β-gal staining indicated that cell senescence was enhanced in MCF-7 cells transfected with sh-HIF1A-AS2 (Figure 3B; $P<0.01$). Taken together, our results indicated that sh-HIF1A-AS2 played an important role in MCF-7 cell proliferation and senescence by regulating miR-548c-3p.

sh-HIF1A-AS2 inhibited cell invasion and EMT by regulating miR-548c-3p in MCF-7 cells

Transwell assay and Western blot were applied to investigate the invasive capacity and EMT process of MCF-7 cells,

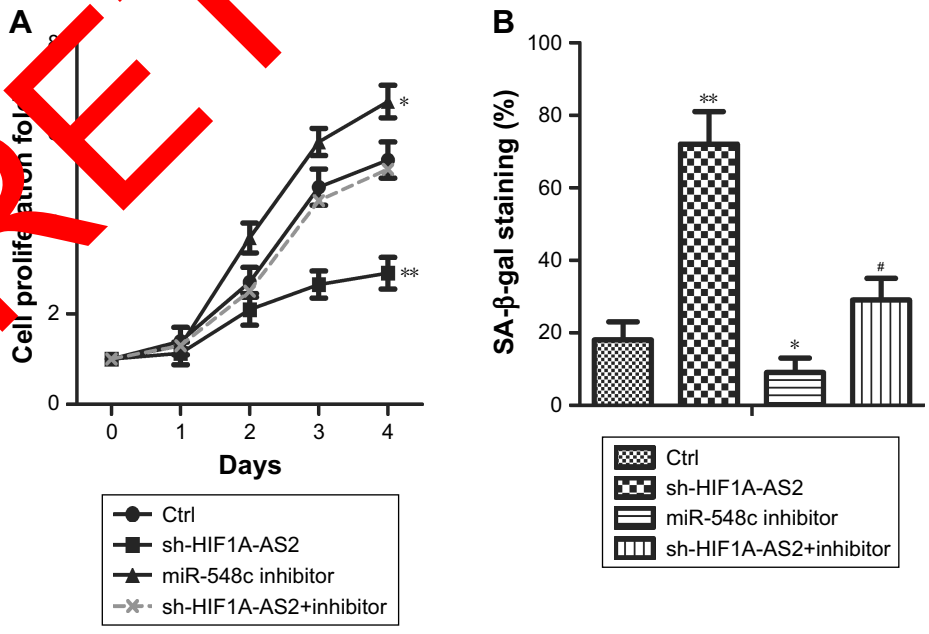

Figure 3 (*Continued*)

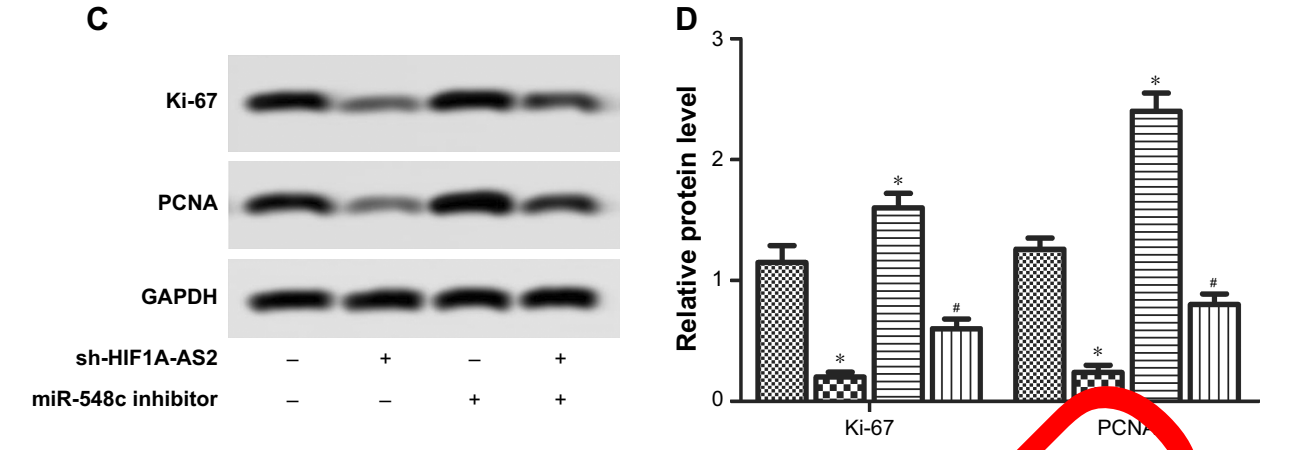

Figure 3 sh-HIF1A-AS2 suppressed proliferation and senescence by regulating miR-548c-3p in MCF-7 cells.
Notes: (**A**) The cell proliferation folds were detected by CCK-8 in MCF-7 cells transfected with sh-HIF1A-AS2 or miR-548c inhibitor and in combination with miR-548c inhibitor (**P*<0.05 vs control, ***P*<0.01 vs control). (**B**) The cell senescence was detected by SA-β-gal staining in MCF-7 cells transfected with sh-HIF1A-AS2 or miR-548c inhibitor and in combination with miR-548c inhibitor (**P*<0.05 vs control, ***P*<0.01 vs control, #*P*<0.05 vs miR-548c inhibitor group). (**C**) The expression of proliferation marker proteins Ki-67 and PCNA were measured by Western blot in MCF-7 cells transfected with sh-HIF1A-AS2 or miR-548c inhibitor and in combination with miR-548c inhibitor. (**D**) Histograms display the statistical analysis of Western blotting results. The bars show mean ± SD of three independent experiments (**P*<0.05 vs control, #*P*<0.05 vs miR-548c inhibitor group).
Abbreviations: CCK-8, Cell Counting Kit-8; Ctrl, control; HIF1A-AS2, hypoxia-inducible factor-1 alpha antisense RNA-2; SA-β-gal, senescence-associated β-galactosidase.

respectively. As shown in Figure 4A, the downregulation of HIF1A-AS2 significantly impeded MCF-7 cell invasion. After transfection with miR-548c-3p inhibitor, the number of invasive cells was significantly increased (Figure 4A, $P<0.05$).

Generally, increase of E-cadherin and decrease of vimentin/N-cadherin expression are the fundamental events in EMT. As shown in Figure 4B, low expression of HIF1A-AS2 observably increased E-cadherin protein level and decreased the

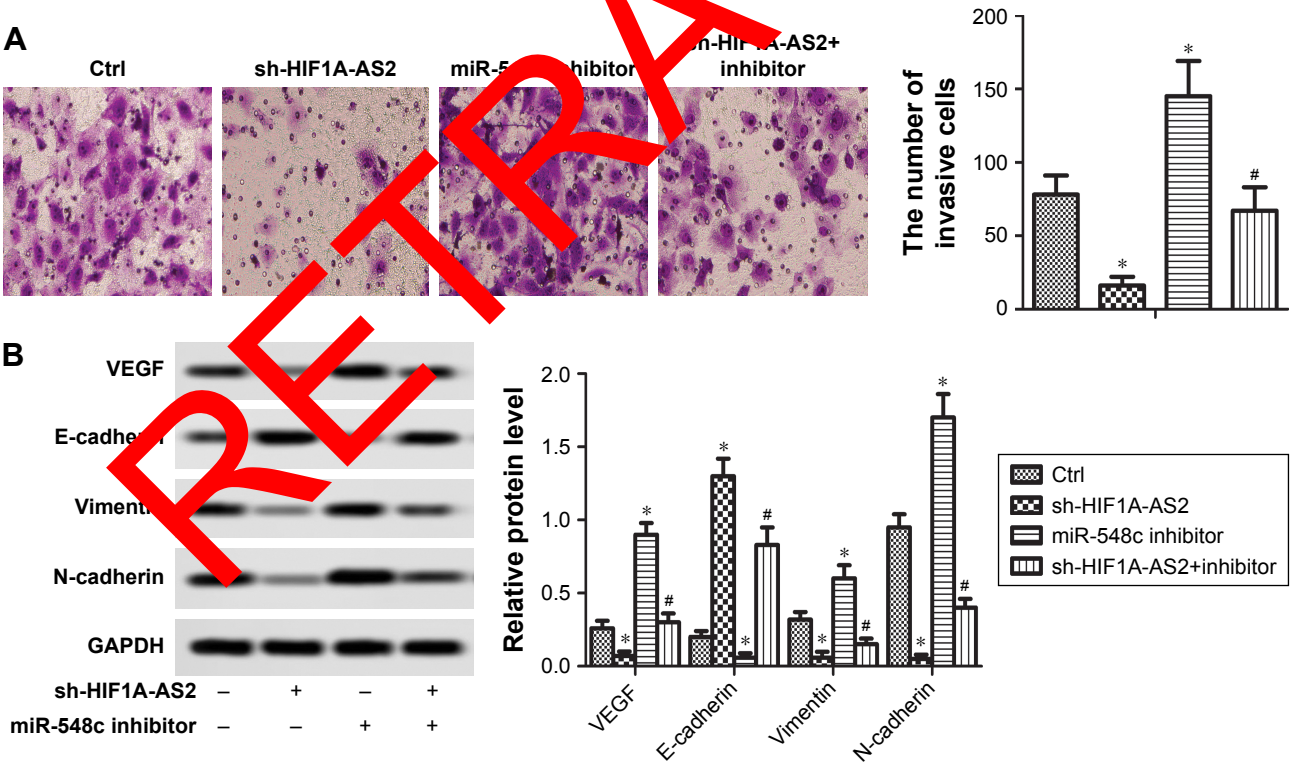

Figure 4 sh-HIF1A-AS2 inhibited cell invasion and epithelial–mesenchymal transition (EMT) by regulating miR-548c-3p in MCF-7 cells.
Notes: (**A**) The invasion ability of MCF-7 cells transfected with sh-HIF1A-AS2 or miR-548c inhibitor and in combination with miR-548c inhibitor was detected by transwell assays. Invasive cells were stained with crystal violet solution, and the quantification of invasive cells is shown (**P*<0.05 vs control, #*P*<0.05 vs miR-548c inhibitor group). (**B**) The expression of EMT marker proteins and VEGF was measured by Western blot in MCF-7 cells transfected with sh-HIF1A-AS2 or miR-548c inhibitor and in combination with miR-548c inhibitor (**P*<0.05 vs control, #*P*<0.05 vs miR-548c inhibitor group).
Abbreviations: Ctrl, control; HIF1A-AS2, hypoxia-inducible factor-1 alpha antisense RNA-2; VEGF, vascular endothelial growth factor.

levels of vimentin and N-cadherin ($P<0.05$), whereas the miR-548c-3p inhibitor showed opposite effects ($P<0.05$). Additionally, the expression of VEGF was significantly restrained in MCF-7 cells with the transfection of sh-HIF1A-AS2. Therefore, our research declared that sh-HIF1A-AS2 restrained cell motility through the inhibitive effect of EMT process via regulating miR-548c-3p in MCF-7 cells.

sh-HIF1A-AS2 inhibited cell motility via regulating HIF-1α/VEGF signaling pathway in MCF-7 cells

To investigate the potential molecular mechanism of sh-HIF1A-AS2 on BC cells, Targetscan7.0 (http://www.targetscan.org), Western blot, and transwell assay were performed. The presumptive target of HIF-1α was shown to be present on miR-548c-3p 3′UTR (wt and mut) (Figure 5A). In addition, the four BC cell lines (MDA-MB-231, MCF-7, ZR-75-1, and BT-549) and MCF-10A were incubated under 1% O_2 for 48 hours, and HIF-1α was measured by RT-qPCR. As shown in Figure 5B, HIF-1α was noticeably upregulated in the four BC cell lines compared with MCF-10A ($P<0.05$, $P<0.01$). Western blot results showed that levels of mesenchymal marker proteins (vimentin), HIF-1α, and VEGF were markedly suppressed in MCF-7 cells transfected with sh-HIF1A-AS2 (Figure 5C, $P<0.05$). However, a reversed result was observed in MCF-7 cells transfected with pLenti-CMV-HIF-1α to overexpress HIF-1α (Figure 5C; $P<0.05$). Besides, knockdown of HIF1A-AS2 by shRNA significantly inhibited invasion, whereas overexpression of HIF-1α had opposite results (Figure 5D and E; $P<0.05$). All these data suggested that sh-HIF1A-AS2 inhibited cell motility via regulating HIF-1α/VEGF signaling pathway in MCF-7 cells.

sh-HIF1A-AS2 inhibited tumor growth and motility by targeting miR-548c-3p to regulate HIF-1α/VEGF pathway in vivo

The in-situ tumor was taken out and weighed 25 days later. As shown in Figure 6, the tumor weight was noticeably reduced in xenograft nude mice injected with MCF-7 cells with sh-HIF1A-AS2 ($P<0.01$), indicating that tumor growth was markedly inhibited in sh-HIF1A-AS2 mice. In addition, RT-qPCR results showed that after subcutaneous injection

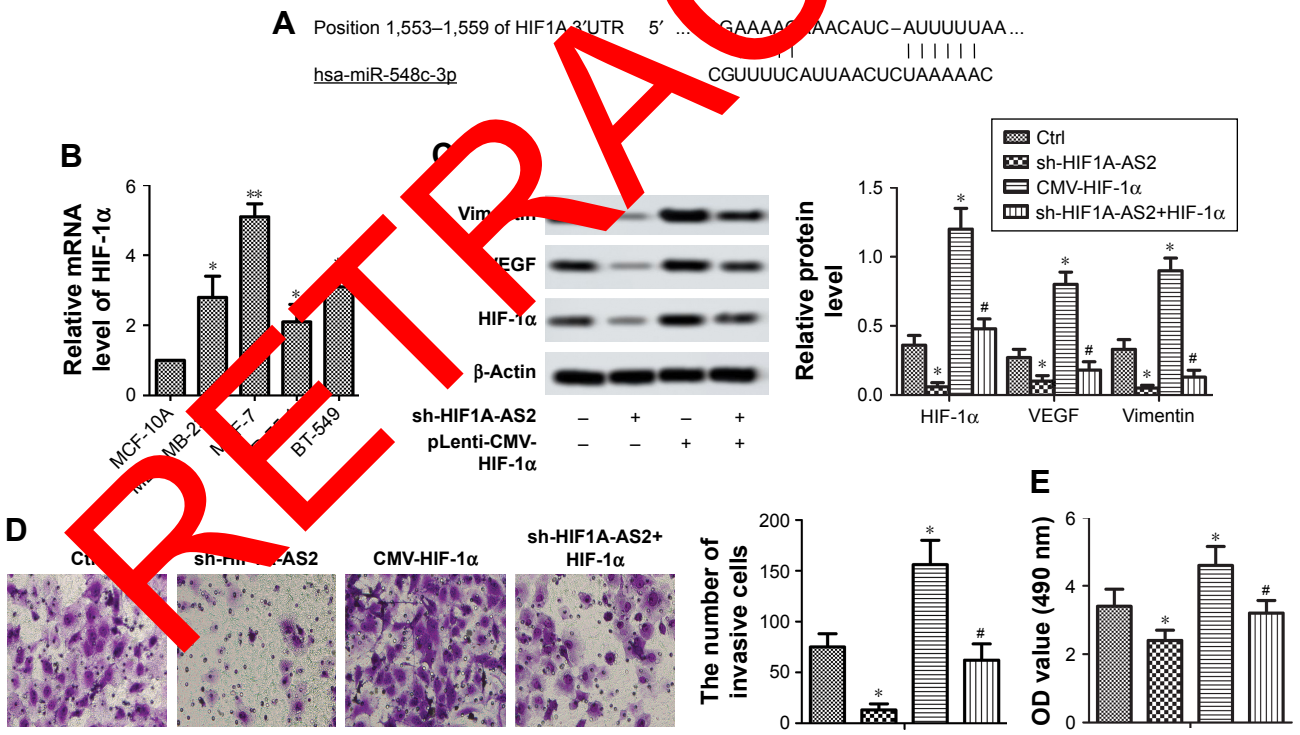

Figure 5 sh-HIF1A-AS2 inhibited cell motility via regulating HIF-1α/VEGF signaling pathway in MCF-7 cells.

Notes: MCF-10A and BC cells lines (MDA-MB-231, MCF-7, ZR-75–1, and BT-549) were incubated under 1% O_2 for 48 hours. (**A**) The target of miR-548c-3p on the HIF1A 3′UTR. (**B**) The expression level of HIF-1α was detected by RT-qPCR (*$P<0.05$ vs control; **$P<0.01$ vs control). (**C**) Expression of EMT marker proteins, VEGF, and HIF-1α was measured by Western blot in MCF-7 cells transfected with sh-HIF1A-AS2 or pLenti-CMV-HIF-1α and in combination with pLenti-CMV-HIF-1α (*$P<0.05$ vs control, #$P<0.05$ vs CMV-HIF-1α group). (**D**) Invasion ability of MCF-7 cells transfected with sh-HIF1A-AS2 or pLenti-CMV-HIF-1α and in combination with pLenti-CMV-HIF-1α. Invasive cells were stained with crystal violet solution, and the quantification of invasive cells is shown (*$P<0.05$ vs control, #$P<0.05$ vs CMV-HIF-1α group). Scale bar =20 μm. (**E**) Proliferation ability was measured by CCK-8 assays in MCF-7 cells transfected with sh-HIF1A-AS2 or pLenti-CMV-HIF-1α and in combination with pLenti-CMV-HIF-1α (*$P<0.05$ vs control, #$P<0.05$ vs CMV-HIF-1α group).

Abbreviations: BC, breast cancer; CCK-8, Cell Counting Kit-8; Ctrl, control; EMT, epithelial -mesenchymal transition; HIF1A-AS2, hypoxia-inducible factor-1 alpha antisense RNA-2; RT-qPCR, quantitative real-time PCR; HIF-1α, hypoxia-inducible factor-1 alpha; UTR, untranslated region; VEGF, vascular endothelial growth factor.

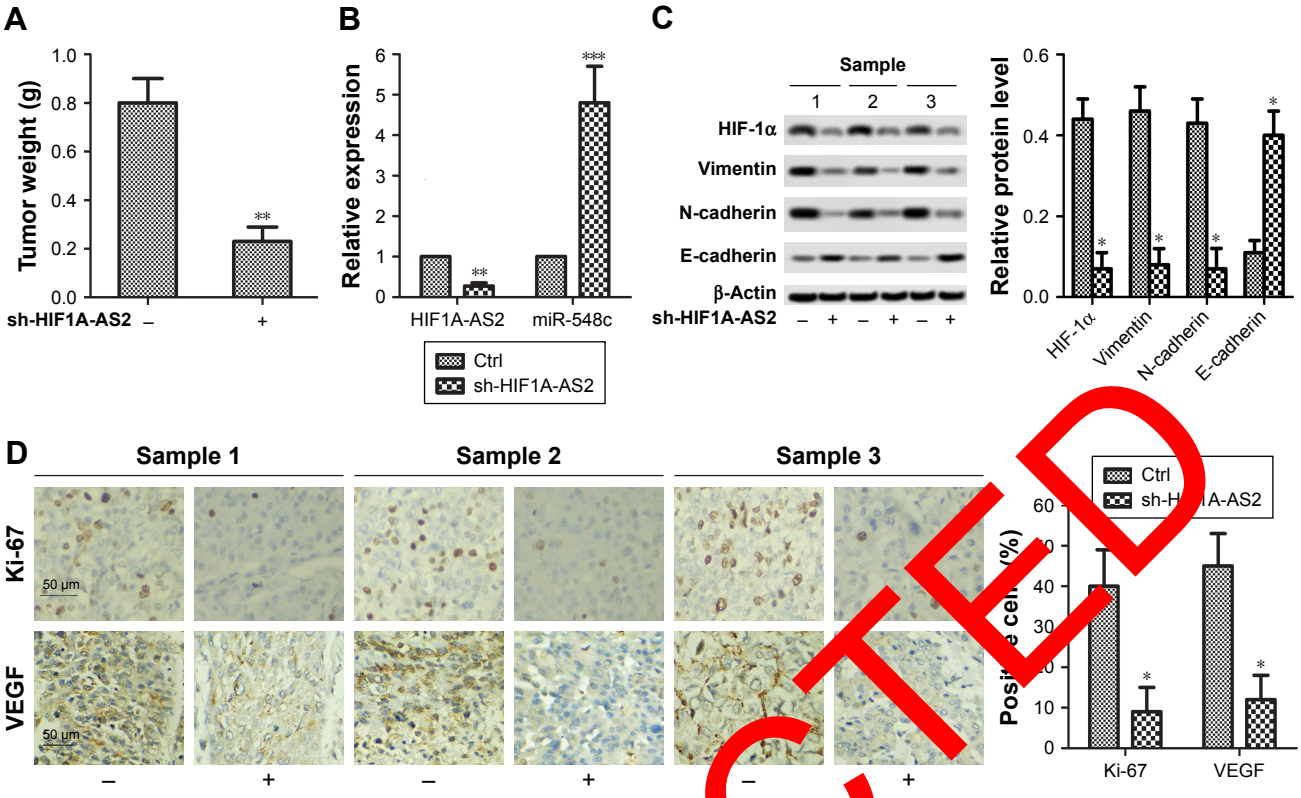

Figure 6 sh-HIF1A-AS2 inhibited tumor growth and motility by targeting miR-548c-3p to regulate HIF-1α/VEGF pathway in vivo.
Notes: (**A**) Tumor weight was noticeably reduced in sh-HIF1A-AS2 group mice (**$P<0.01$ vs control). (**B**) Expression level of miR-548c-3p was detected by RT-qPCR in sh-HIF1A-AS2 group mice (**$P<0.01$ vs control; ***$P<0.001$ vs control). (**C**) Expression of EMT marker proteins and HIF-1α was measured by Western blot in sh-HIF1A-AS2 group mice (*$P<0.05$ vs control). (**D**) Expression of proliferation marker protein Ki-67 and VEGF in formalin-fixed, paraffin-embedded tumors from sh-HIF1A-AS2 group mice was detected by IHC analysis (*$P<0.05$ vs control). "–" stands for Ctrl group and "+" stands for sh-HIF1A-AS2 group.
Abbreviations: Ctrl, control; EMT, epithelial -mesenchymal transition; HIF-1α, hypoxia-inducible factor-1 alpha; HIF1A-AS2, hypoxia-inducible factor-1 alpha antisense RNA-2; IHC, immunohistochemistry; RT-qPCR, quantitative real-time PCR; VEGF, vascular endothelial growth factor.

of MCF-7 cells with sh-HIF1A-AS2 a large amount of miR-548c-3p was accumulated in xenograft nude mice (Figure 6B; $P<0.001$). In addition, expression of EMT marker proteins and HIF-1α was measured by Western blot in sh-HIF1A-AS2 group mice. As shown in Figure 6C, knockdown of HIF1A-AS2 by siRNA significantly inhibited the expression of mesenchymal marker proteins (vimentin and N-cadherin), and promoted the expression of epithelial marker protein (E-cadherin) ($P<0.05$). Furthermore, IHC analysis results demonstrated that the expression of Ki-67 and VEGF was reduced in formalin-fixed, paraffin-embedded tumors from sh-HIF1A-AS2 group mice (Figure 6D; $P<0.05$). Thus, we concluded that sh-HIF1A-AS2 inhibited tumor growth and motility by targeting miR-548c-3p to regulate HIF-1α/VEGF pathway in vivo.

Discussion

As a delegate of the most common cancer among woman, BC has been increasing in morbidity worldwide.[27,28] Although various therapies are available, the survival rates of BC patients remain low.[7] Additionally, chemoresistance and adverse reactions extremely impeded the therapeutic effect of BC treatment.[29,30] Up to now, no treatment that is completely effective is available. The abnormally expressed proteins that were associated with increased proliferation and motility of cells were regarded as culprits in the development of BC.[31,32] Therefore, analyzing the underlying molecular mechanism is the most intuitive way for the treatment of BC.

As a hypoxia-dependent lncRNA, HIF1A-AS2 has been reported to be correlated with a variety of cancers. It was first found to be abnormally expressed in nonpapillary clear cell renal carcinomas.[33] Subsequently, HIF1A-AS2 was proved to be involved in the progression, such as proliferation, migration, and apoptosis of various cancers. Chen et al revealed that overexpression of HIF1A-AS2 promoted cell proliferation, tumor invasion, and lymph node metastasis in gastric cancer[16] and bladder cancer.[17] With the deepening of research, Li et al reported that HIF1A-AS2 accelerated cell viability, migration, and tube formation by activating HIF-1α/VEGF/Notch1 cascade pathways in human umbilical vein endothelial

cells.[18] Besides, HIF1A-AS2 also exerted carcinogenicity in colorectal cancer, thus demonstrating that HIF1A-AS2 might be used as a therapeutic target in colorectal cancer.[19] Similarly in our study, we found that HIF1A-AS2 played an analogous role in BC and that sh-HIF1A-AS2 remarkably impeded proliferation, invasion, and EMT in vitro and vivo.

miR-548c-3p is a pivotal small RNA molecule involved in cell proliferation, invasion, and tumorigenesis. Studies have shown that miR-548c-3p is widely present in human embryonic stem cells and unfractionated castration-resistant prostate cancer.[23] Luo et al elucidated that overexpression of miR-548c-3p remarkably suppressed cell viability and promoted apoptosis and G2/M cell cycle arrest.[33] In addition, miR-548c-3p was also reported to be involved in the inhibitive effect of glioma tissue cell proliferation and migration in vitro.[29] According to the report of Tormo et al, miR-548c-3p suppressed doxorubicin-treated MCF-7 cell viability in BC.[26] Consistent with these results, in our study, we manifested that overexpression of HIF1A-AS2 significantly inhibited the expression of miR-548c-3p, while knockdown of HIF1A-AS2 markedly elevated miR-548c-3p level. The enhanced miR-548c-3p levels restrained proliferation, invasion, and EMT, and promoted cell senescence in MCF-7 cells and tumor tissue.

As an oxygen-sensitive transcription factor, HIF-1α activates transcription of various proangiogenic cytokines such as VEGF. Studies have shown the critical role of HIF-1α/VEGF pathway in angiogenesis[21,34,35] and tumorigenesis. Previous studies demonstrated that the breast tumor proliferation was inhibited by simvastatin via targeting the AMPK/HIF-1α/VEGF signaling pathway.[34] Besides, research by Kim and Ma also suggested that Maponticin markedly suppressed the angiogenic and metastatic activities by targeting the HIF-1α/VEGF signaling pathway.[36] In addition, a novel signaling pathway mTOR/HIF-1α/VEGF involved in the inhibitive effect of glioma cell proliferation and invasion was found by Nan et al.[37] Moreover, the expression of HIF-1α also lead to increased VEGF-A and activation of HIF-1α/VEGF signaling pathway in lung cancer cells.[38] Similarly, in our research, we first demonstrated that sh-HIF1A-AS2 represses HIF-1α/VEGF signaling pathway to impede the BC cell proliferation, senescence, invasion, and angiogenesis by targeting miR-548c-3p in vitro and vivo.

Conclusion

In conclusion, our research revealed a novel mechanism of HIF1A-AS2 action in tumorigenesis of BC. The primary mechanisms can be summarized as following: 1) HIF1A-AS2 was upregulated in BC cells and tumor, while miR-548c-3p was downregulated. In addition, sh-HIF1A-AS2 noticeably enhanced the expression of miR-548c-3p in cells and tumor, that is, HIF1A-AS2 has a negative regulation on miR-548c-3p. 2) sh-HIF1A-AS2 noticeably reduced the cell proliferation, invasion, and angiogenesis in cells and tumor. 3) sh-HIF1A-AS2 interacted with miR-548c-3p to inhibit the tumor growth and motility via interfering the HIF-1α/VEGF pathway in vitro and vivo.

Acknowledgment

Xiao Guo and Shenghai Lee are co-first authors for this study.

Author contributions

XG, SL, and PC conceived and designed this study, were involved in the animal assay and statistical analysis, carried out the cell line-based research, wrote the manuscript, and revised the manuscript. PC provided useful input for the analyses and helped in editing the manuscript. All authors read and approved the final manuscript and agree to be accountable for all aspects of the work in ensuring that questions related to the accuracy or integrity of any part of the work are appropriately investigated and resolved.

Disclosure

The authors report no conflicts of interest in this work.

References

1. Torre L, Bray F, Siegel R, et al. Global cancer statistics, 2012. *CA Cancer J Clin*. 2015;65(2):87–108.
2. Jaffee EM, Dang CV, Agus DB, et al. Future cancer research priorities in the USA: a Lancet oncology Commission. *Lancet Oncol*. 2017;18(11):e653–e706.
3. Chen W, Zheng R, Baade PD, et al. Cancer statistics in China, 2015. *CA Cancer J Clin*. 2016;66(2):115–132.
4. Sosa MS, Bragado P, Aguirre-Ghiso JA. Mechanisms of disseminated cancer cell dormancy: an awakening field. *Nat Rev Cancer*. 2014;14(9):611–622.
5. Pantel K, Brakenhoff RH. Dissecting the metastatic cascade. *Nat Rev Cancer*. 2004;4(6):448–456.
6. Gonzalez-Angulo AM, Morales-Vasquez F, Hortobagyi GN. Overview of resistance to systemic therapy in patients with breast cancer. *Adv Exp Med Biol*. 2007;608(1):1.
7. Kolahdooz F, Jang SL, Corriveau A, Gotay C, Johnston N, Sharma S. Knowledge, attitudes, and behaviours towards cancer screening in Indigenous populations: a systematic review. *Lancet Oncol*. 2014;15(11):e504–e516.
8. Pusztai L, Karn T, Safonov A, Abu-Khalaf MM, Bianchini G. New strategies in breast cancer: immunotherapy. *Clin Cancer Res*. 2016;22(9):2105–2110.
9. Guttman M, Rinn JL. Modular regulatory principles of large non-coding RNAs. *Nature*. 2012;482(7385):339–346.
10. Khalil M, Guttman M, Huarte M, et al. Many human large intergenic noncoding RNAs associate with chromatin-modifying complexes and affect gene expression. *Proc Natl Acad Sci USA*. 2009;106(28):11667–11672.
11. Yu G, Yao W, Gumireddy K, et al. Pseudogene PTENP1 functions as a competing endogenous RNA to suppress clear-cell renal cell carcinoma progression. *Mol Cancer Ther*. 2014;13(12):3086–3097.

12. Yan Y, Han J, Li Z, Yang H, Sui Y, Wang M. Elevated RNA expression of long non-coding HOTAIR promotes cell proliferation and predicts a poor prognosis in patients with diffuse large B cell lymphoma. *Mol Med Rep*. 2016;13(6):5125–5131.
13. Ying L, Chen Q, Wang Y, Zhou Z, Huang Y, Qiu F. Upregulated MALAT-1 contributes to bladder cancer cell migration by inducing epithelial-to-mesenchymal transition. *Mol Biosyst*. 2012;8(9):2289–2294.
14. Thrash-Bingham CA, Tartof KD. A HIF: a natural antisense transcript overexpressed in human renal cancer and during hypoxia. *J Natl Cancer Inst*. 1999;91(2):143–151.
15. Bertozzi D, Iurlaro R, Sordet O, Marinello J, Zaffaroni N, Capranico G. Characterization of novel antisense HIF-1α transcripts in human cancers. *Cell Cycle*. 2011;10(18):3189–3197.
16. Chen WM, Huang MD, Kong R, et al. Antisense long noncoding RNA HIF1A-AS2 is upregulated in gastric cancer and associated with poor prognosis. *Dig Dis Sci*. 2015;60(6):1655–1662.
17. Chen M, Zhuang C, Liu Y, et al. Tetracycline-inducible shRNA targeting antisense long non-coding RNA HIF1A-AS2 represses the malignant phenotypes of bladder cancer. *Cancer Lett*. 2016;376(1):155–164.
18. Li L, Wang M, Mei Z, et al. lncRNAs HIF1A-AS2 facilitates the upregulation of HIF-1α by sponging to miR-153-3p, whereby promoting angiogenesis in HUVECs in hypoxia. *Biomed Pharmacother*. 2017;96:165–172.
19. Lin J, Shi Z, Yu Z, He Z. LncRNA HIF1A-AS2 positively affects the progression and EMT formation of colorectal cancer through regulating miR-129-5p and Dnmt3a. *Biomed Pharmacother*. 2018;98:433–439.
20. Cotran R, Kumar V, Robbins S. *Robbins and Cotran Pathologic Basis of Disease* [e-book]. 9th edition. 2010.
21. Wang J, Li G, Wang Y, et al. Suppression of tumor angiogenesis by metformin treatment via a mechanism linked to targeting of HER2/HIF-1α/VEGF secretion axis. *Oncotarget*. 2015;6(42):44579–44592.
22. Li LJ, Huang Q, Zhang N, Wang GB, Liu YH. miR-376b-5p regulates angiogenesis in cerebral ischemia. *Mol Med Rep*. 2014;10(1):527–5
23. Rane JK, Scaravilli M, Ylipää A, et al. MicroRNA expression prof of primary prostate cancer stem cells as a source of biomarkers an therapeutic targets. *Eur Urol*. 2015;67(1):7–10.
24. Lu J, Zhang M, Yang X, Cui T, Dai J. MicroRNA-5 c-3p hibits T98G glioma cell proliferation and migration by dow egulating Myb. *Oncol Lett*. 2017;13(5):3866–3872.
25. Chang H, Kim N, Park JH, et al. Different mi RNA ion levels in gastric cancer depending on *Helicobact ylori* infec *Gut Liver*. 2015;9(2):188–196.
26. Tormo E, Pineda B, Serna E, et al. Mic NA pr e in response t oxoru-bicin treatment in breast cancer. *J ell Biochem*. 20 116(9):2061–2073.
27. McGuire A, Brown JA, Malone C, McLaughlin R, Kerin MJ. Effects of age on the detection and management of breast cancer. *Cancers*. 2015;7(2):908–929.
28. Zahmatkesh B, Keramat A, Alavi N, et al. Breast cancer trend in Iran from 2000 to 2009 and prediction till 2020 using a trend analysis method. *Asian Pac J Cancer Prev*. 2016;17(3):1493–1498.
29. Szakács G, Paterson JK, Ludwig JA, Booth-Genthe C, Gottesman MM. Targeting multidrug resistance in cancer. *Nat Rev Drug Discov*. 2006;5(3):219–234.
30. Kars MD, Işeri OD, Gunduz U, Molnar J. Reversal of multidrug resistance by synthetic and natural compounds in drug-resistant MCF-7 cell lines. *Chemotherapy*. 2008;54(3):194–200.
31. Yang YX, Wei L, Zhang YJ, et al. Long non-coding RNA p10247, high expressed in breast cancer (lncRNA-BCHE), is correlated with metastasis. *Clin Exp Metastasis*. 2018;35(3):1 121.
32. Song R, Zhang J, Huang J, Hai T, Huang Long n-coding RNA GHET1 promotes human breast can cell prolife on, invasion and migration via affecting epithelial n enchymal trans on. *Cancer Biomark*. 2018;22(3):565–573.
33. Luo Z, Li D, Luo X, et al. E creased expre on of R-548c-3p in osteosarcoma contribute cell pro eration rgeting ITGAV. *Cancer Biother Radiopha* . 201 1(5):153–158.
34. Wang JC, Li XX, ctivation AMPK by simvastatin inhibited breast mor angio sis via peding HIF-1α-induced pro-angioge r. *Cancer Sci* ;109(5):1627–1637.
35. Ni X, Zha , Ma J, al. Hypoxia-induced factor-1 alpha upregulates vascular endothelial gr th factor C to promote lymphangiogenesis and genesis in breast cer patients. *J Biomed Res*. 2013;27(6):4 –485.
36. m A, Ma JY. aponticin decreases the metastatic and angiogenic ilities of cance ells via suppression of the HIF-1α pathway. *Int J O l*. 2018;53(1160–1170.
37. Nan , Guo L, et al. miRNA-451 inhibits glioma cell roliferation and invasion through the mTOR/HIF-1α/VEGF signaling pa by targeting Cab39. *Hum Gene Ther Clin Dev*. 2018;29(3):156–166.
38. Zhu H, Zhang S. Hypoxia inducible factor-1α/vascular endothelial growth factor signaling activation correlates with response to radiotherapy and its inhibition reduces hypoxia-induced angiogenesis in lung cancer. *J Cell Biochem*. 2018;119(9):7707–7718.